Collaborative Navigation in Urban Environments via GNSS and 5G Signals

Yuan Zhang, Rui Wang, and Zhe Xing
College of Electronics and Information Engineering, Tongji University, Shanghai China
yuanzhang@tongji.edu.cn, ruiwang@tongji.edu.cn, zxing@tongji.edu.cn

***Abstract*—In this paper, we address the key enabling technologies for collaborative global navigation satellite system/fifth generation (GNSS/5G) navigation in urban environments. First, we derive the posterior belief over the state space conditioned on the given ranging measurements in non-ideal ranging environment (e.g., line-of-sight/non-line-of-sight (LOS/NLOS)) and GNSS velocity. Then, building on the premises of non-ideal ranging in LOS/NLOS, a robust particle filter (RPF) algorithm adopted for urban environments is proposed to estimate the sight state and position of the mobile terminal (MT). Statistics on 5G measurement error in a LOS environment and in the presence of NLOS are presented. Finally, comprehensive performance evaluations are carried out in 5G ultra-dense networks. Simulation results demonstrate that meter-scale positioning and tracking accuracy can be achieved in LOS/NLOS using the proposed RPF technique.**

***Index Terms*—Collaborative navigation, robust particle filter (RPF), line-of-sight/non-line-of-sight (LOS/NLOS), urban environments**

I. Introduction

The fifth-generation (5G) communication networks require highly-accurate knowledge of mobile terminal (MT) to enhance location-based services, such as autopilot [1], [2], pedestrian navigation [3], [4], etc. The existing positioning technologies, such as Bluetooth, WiFi, which all yield positioning accuracy in the range of a few meters, as well as global navigation satellite system (GNSS) [5] based solutions in which the accuracy of single point positioning (SPP) is in the order of 10 meters at best. The order of one meter or even below is envisaged for future accurate positioning services of 5G wireless communication networks [6].

5G positioning has been extensively studied in different contexts. A joint device positioning and clock synchronization scheme in 5G ultra-dense networks was proposed in [7]. A novel tensor-based method was presented in [8] for channel estimation that allowed estimation of mmWave channel parameters in a non-parametric form, in turn enabled positioning and mapping using only diffuse multipath. A new method was proposed in [9] for cooperative vehicle positioning and mapping of the radio environment, comprising a multiple-model probability hypothesis density filter and a map fusion routine, which considered different types of objects and different fields of view. [10] described how centimeter-level localization accuracy can be achieved, particularly through the use of map-based techniques. An integrated methodology of GNSS and device to device (D2D) measurements in the 5G communication system was introduced in [11].

Cellular positioning technique in urban environments is a challenging task due to presence of NLOS propagation in 5G ultra-dense networks. NLOS occurs due to the reflection and refraction of radio signals, which introduces a positive bias with the LOS condition, thus, leading to degradation of positioning accuracy. In addition, NLOS arises from the propagation of radio signals in many communication systems (e.g., fourth-generation (4G), 5G, etc.). NLOS propagation is likely to occur in the 5G communication system, which brings challenges to meet the needs of high-precision positioning, especially in the field of autonomous ground vehicle (AGV), pedestrian navigation, etc. Several 5G positioning estimation algorithms for NLOS were proposed in [12], [13]. Dynamic BS formation for solving NLOS problems in 5G millimeter-wave communication was introduced in [12]. A cooperative localization algorithm was developed in [13] for mixed LOS/NLOS environments where the NLOS effect was mitigated by exploiting the geometric relationship of range biases.

In this paper, building on the premises of 5G high-accuracy positioning and LOS/NLOS propagation conditions, we develop e key enabling technologies for GNSS/5G collaborative navigation in urban environments, where a robust particle filter (RPF) technique is proposed for state estimation of the MT.

More specifically, the novelty and technical contributions of this paper are summarized as follows:

- We derive the posterior belief over the state space conditioned on the given ranging measurements in non-ideal ranging environments (e.g., LOS/NLOS) and GNSS velocity.
- Considering the derived posterior distribution, a robust particle filter (RPF) algorithm for non-ideal ranging in LOS/NLOS scenarios is proposed to estimate the sight state and position of the MT.
- 5G measurement error statistics in a LOS environment and in the presence of NLOS are presented.
- We considered the interacting multiple model-extended Kalman filter (IMM-EKF) [14], and compared it with

ICC 2023 - IEEE International Conference on Communications | 978-1-5386-7462-8/23/$31.00 ©2023 IEEE | DOI: 10.1109/ICC45041.2023.10279482

our proposed RPF algorithm in a mixed LOS/NLOS model.

The remainder of this paper is organized as follows. Section II proposes a GNSS/5G collaborative navigation scheme based on a RPF technique. Section III evaluates the performance of the proposed methodology. Section IV draws the conclusions.

II. The proposed RPF Technique for GNSS/5G Collaborative Navigation

The performance of RPF technology is evaluated in 5G ultra dense network scenarios, which mainly include two types of BSs: Urban Macro (UMa) BS and Urban Micro (UMi) BS. According to [15], 5G ultra-dense network scenarios, in which the simulation methodology is specified by the 3GPP working group, are defined using predefined communication network parameters.

We consider the scenario that the MT navigating in urban environments can obtain ranging measurements $\mathbf{y}_{\mathrm{MB}} = (d^1_{\mathrm{MB},t}, ..., d^{\mathcal{M}}_{\mathrm{MB},t})$ at time instant t between $\mathcal{M}$ BSs and the MT. The MT is characterized by the state vector $\mathbf{s}_t$ and $\mathbf{n}_t$, where $\mathbf{s}_t = (x_{\mathrm{MT},t}, y_{\mathrm{MT},t})$ is the 2D position of the MT, and $\mathbf{n}_t = (s^1_{\mathrm{MT},t}, ..., s^{\mathcal{M}}_{\mathrm{MT},t})$ denotes the sight state in LOS/NLOS in which $s^i_{\mathrm{MT},t} = 1$ for LOS and $s^i_{\mathrm{MT},t} = 0$ for NLOS.

A. Pseudorange Measurement Model

The ranging measurement model between the MT and BS_i is given by

$$d^i_{\mathrm{MB},t} = \bar{d}^i_{\mathrm{MB},t} + v^i_1 + (1 - s^i_{\mathrm{MT},t}) \times v^i_2, \tag{1}$$

where $\bar{d}^i_{\mathrm{MB},t}$ denotes the true distance measurement, v^i_1 is a zero-mean Gaussian noise following $v^i_1 \sim \mathcal{N}(0, \sigma^2_{v_1})$, and v^i_2 denotes a positive distance bias induced by the blockage of direct path [16], [17]. Normally, v^i_1 and v^i_2 are independent.

For each BS_i, the sight state of the MT can be dynamically updated by [18]

$$s^i_{\mathrm{MT},t} = \begin{cases} 1, & \text{if}(p(s^i_{\mathrm{MT},t} = 1 | s^i_{\mathrm{MT},t-1})) \times p^i_t > p_{\mathrm{threshold}} \\ 0, & \text{else} \end{cases}, \tag{2}$$

where $p_{\mathrm{threshold}}$ is the NLOS identification threshold. In 5G ultra dense network scenarios, the MT is assumed to be moving continuously. The current sight state and the last sight state are not independent with each other, i.e., the current sight state is defined by the last sight state and the current obversation likelihood. $p(s^i_{\mathrm{MT},t} = 1 | s^i_{\mathrm{MT},t-1})$ is transition probability for predicting the current sight state from the last state using first-order Markov given by

$$\begin{cases} p(s^i_{\mathrm{MT},t} = 1 | s^i_{\mathrm{MT},t-1} = 1) = b \\ p(s^i_{\mathrm{MT},t} = 0 | s^i_{\mathrm{MT},t-1} = 1) = 1 - b \\ p(s^i_{\mathrm{MT},t} = 0 | s^i_{\mathrm{MT},t-1} = 0) = b \\ p(s^i_{\mathrm{MT},t} = 1 | s^i_{\mathrm{MT},t-1} = 0) = 1 - b \end{cases}, \tag{3}$$

where b is the transition probability of LOS that may depend on the urban environment, and the LOS state likelihood function is given by

$$p^i_t = \begin{cases} \frac{1}{\sqrt{2\pi}\sigma_{v^i_1}} \exp\left(-\frac{(d^i_{\mathrm{MB},t} - \tilde{d}^i_{\mathrm{MB},t})^2}{2\sigma^2_{v^i_1}} \right), & \text{if } (d^i_{\mathrm{MB},t} > \tilde{d}^i_{\mathrm{MB},t}) \\ 1, & \text{else} \end{cases}, \tag{4}$$

where $\tilde{d}^i_{\mathrm{MB},t} = \bar{d}^i_{\mathrm{MB},t} + a$ is the ideal ranging.

B. Linear Model for the State Transition with GNSS Control

With the RPF, the obtained ranging measurements are used to estimate the MT position as well as the sight states. Thus, the state of the process is defined as

$$\mathbf{X}(t) = [x_{\mathrm{MT},t}, y_{\mathrm{MT},t}, s^1_{\mathrm{MT},t}, ..., s^{\mathcal{M}}_{\mathrm{MT},t}]^{\mathrm{T}} \in \mathbb{R}^{2+\mathcal{M}}. \tag{5}$$

Considering the presence of an input control with sampling period Δt, the linear model for the state transition can be extended as follows

$$\mathbf{s}_t = \mathbf{F}\mathbf{s}_{t-1} + \mathbf{B}\mu_{t-1} + \mathbf{w}_{t-1}, \tag{6}$$

where the state transition matrix $\mathbf{F} \in \mathbb{R}^{2\times 2}$ is a 2×2 identity matrix, the control input matrix $\mathbf{B} \in \mathbb{R}^{2\times 2}$ is

$$\mathbf{B} = \begin{bmatrix} \Delta t & 0 \\ 0 & \Delta t \end{bmatrix}. \tag{7}$$

The linear model for the state transition can be applied to collaborative navigation, provided that μ includes external inputs that control the MT movement, where the control is assumed to be the velocity v_{G} introduced by GNSS module. The process noise, of size 2×1, $\mathbf{w}$ is assumed to be a zero-mean Gaussian noise following $\mathbf{w} \sim \mathcal{N}(0, \mathbf{Q})$, where the convariance matrix $\mathbf{Q}$ described the uncertainty of the state.

C. RPF for GNSS/5G Collaborative Navigation

The significance of GNSS/5G collaborative navigation is to estimate a posterior distribution over state space conditioned on the measurements. For GNSS/5G collaborative navigation, we distinguish two types of measurement information: 1) perceptual measurement information such as ranging measurements $d^i_{\mathrm{MB},t}$ of the MT, 2) GNSS data $y_{\mathrm{G},t}$ of the MT, which carry information about velocity of the MT. Then, we have

$$bel\left(\mathbf{s}_t\right) = p\left(\mathbf{s}_t | O^i_t, y_{\mathrm{G},t-1}, O^i_{t-1}, y_{\mathrm{G},t-2}, ..., O^i_1\right), \forall i \in \mathcal{M}. \tag{8}$$

where $O^i_{1:t}$ denotes the measurement information starting at time 1 up to time t.

The recursive equation is obtained as

$$bel\left(\mathbf{s}_t\right)=\frac{p(O_t^i|\mathbf{s}_t)\int p(\mathbf{s}_t|\mathbf{s}_{t-1},y_{\mathrm{G},t-1})bel(\mathbf{s}_{t-1})d_{\mathbf{s}_{t-1}}}{p(O_t^i|y_{\mathrm{G},t-1},...,O_1^i)}. \tag{9}$$

The pair $\left\langle \mathbf{s}_t^j,\mathbf{s}_{t-1}^j\right\rangle$ is distributed according to

$$q_t=p(\mathbf{s}_t^j|\mathbf{s}_{t-1}^j,y_{\mathrm{G},t-1})\times bel\left(\mathbf{s}_{t-1}^j\right), \tag{10}$$

where the prior distribution q_t is to propose samples of the desired posterior distribution.

Considering the pseudorange observation $d_{\mathrm{MB},t}^i$ and the sight state $s_{\mathrm{MT},t}^i$ in LOS/NLOS environment, we build the feasible region to filter the particles outside the intersection of the multiple circular areas. The feasible region is defined as

$$D_{\mathrm{NLOS}}=\left\{\mathbf{s}_t|\left\|\mathbf{s}_t-\mathbf{s}_{\mathrm{BS}_i}\right\|\le d_{\mathrm{MB},t}^i,i=1,...,\mathcal{L}\right\}, \tag{11}$$

where $\mathbf{s}_{\mathrm{BS}_i}$ is the position of the BS_i, $\left\|\mathbf{s}_t-\mathbf{s}_{\mathrm{BS}_i}\right\|$ is the Euclidean distance between $\mathbf{s}_t$ and $\mathbf{s}_{\mathrm{BS}_i}$, and $\mathcal{L}$ represents the highest sequence number of the detected NLOS measurements.

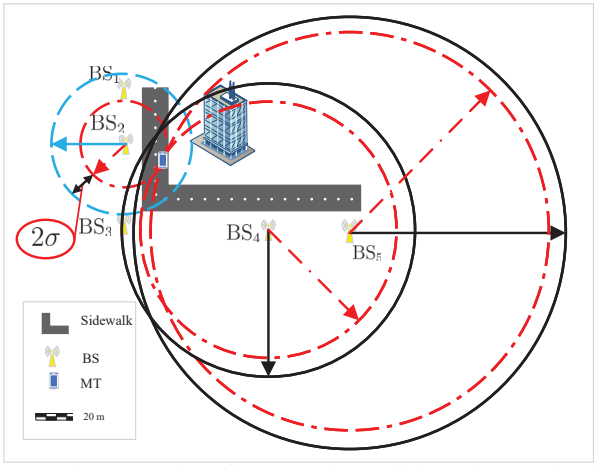

Fig. 1: The scenario of GNSS/5G collaborative navigation with LOS/NLOS environment.

The scenario of GNSS/5G collaborative navigation with LOS/NLOS environment in 5G ultra-dense networks is as shown in Fig. 1. In this scenario, the measured diatances are denoted as solid circles, and true diatances are represented by red dashed circles. For LOS measurements (e.g., BS_2), the measured distance and the true diatance are represented by the red dashed circle. The feasible region D that consists of NLOS measurements from BS_4 and BS_5 is partly large. Thus, LOS measurements are considered to build the feasible region D_{LOS}, and the feasible region D_{LOS} is given by

$$D_{\mathrm{LOS}}=\left\{\mathbf{s}_t|\left\|\mathbf{s}_t-\mathbf{s}_{\mathrm{BS}_i}\right\|\le d_{\mathrm{MB},t}^i+2\sigma_{v_1^i},i=1,...,\mathcal{K}\right\}, \tag{12}$$

where $\mathcal{K}$ represents the highest sequence number of the detected LOS measurements. Thus, the enhanced feasible region D is denoted as

$$D=D_{\mathrm{NLOS}}\cap D_{\mathrm{LOS}}. \tag{13}$$

Considering the enhanced feasible region D to filter the particles, the particle weights are updated as follows

$$\omega_t^j=\begin{cases}\omega_t^j, & \text{if } \left(\mathbf{s}_t^j\in D\right)\\ 0, & \text{else}\end{cases}. \tag{14}$$

Restate the desired distribution for the sample pair $\left\langle \mathbf{s}_t^j,\mathbf{s}_{t-1}^j\right\rangle$ given by

$$bel(\mathbf{s}_t^j)=\frac{p(O_t^i|\mathbf{s}_t^j)p(\mathbf{s}_t^j|\mathbf{s}_{t-1}^j,y_{\mathrm{G},t-1})bel(\mathbf{s}_{t-1}^j)}{p(O_t^i|y_{\mathrm{G},t-1},...,O_1^i)}. \tag{15}$$

Since $p(O_t^i|y_{\mathrm{G},t-1},...,O_1^i)$ is a constant, the weights of the particles are derived as

$$\omega_t^j=\frac{p(O_t^i|\mathbf{s}_t^j)}{p(O_t^i|y_{\mathrm{G},t-1},...,O_1^i)}\propto p(O_t^i|\mathbf{s}_t^j). \tag{16}$$

For the LOS measurements, the observation likelihood of the jth particle is denoted as

$$p(O_t^i|\mathbf{s}_t^j)=\left(\prod_{i=1}^{\mathcal{L}}p_t^{ji}\right)^{\frac{1}{\mathcal{L}}}, \tag{17}$$

where p_t^{ji} denotes the likelihood of achieving the measurements $d_{\mathrm{MB},t}^i$ with the BS_i by the jth particle, we have

$$p_t^{ji}=\frac{1}{\sqrt{2\pi}\sigma_{v_1^i}}\exp\left(-\frac{(d_{\mathrm{MB},t}^i-\tilde{d}_{\mathrm{MB},t}^{ji})^2}{2\sigma_{v_1^i}^2}\right). \tag{18}$$

III. Simulation Resluts

In this section, comprehensive numerical evaluations are examined to illustrate and quantify the achievable GNSS/5G collaborative navigation performance using RPF in 5G ultra-dense networks. UMi-street and UMa-street scenarios in 5G ultra-dense networks are shown in Fig. 2. The deployment area has plane area of $60\,\mathrm{m}\times 110\,\mathrm{m}$. GNSS data are obtained by adding Gaussian noises to the ideal constant velocity $v_{\mathrm{G}}=1\,\mathrm{m/s}$, while 5G ranging information is generated by additional measurement noise (cf.(19)) and NLOS bias is modeled according to (21). The noise distribution of the GPS receiver is determined by a GPS receiver module. Here, the GPS receiver module we use is the Garmin GPS 18x-5Hz with position error $2\sigma_{gnss}<15\,\mathrm{m}$ (where σ_{gnss} denotes the standard deviation of the positioning), velocity error $0.1\,\mathrm{knot}$ and frequency $5\,\mathrm{Hz}$ [19].

Four algorithms are compared in this section: IMM-EKF, PF [20], RPF using GNSS and 5G cellular signals, and GNSS solutions. The parameters $P_{\mathrm{threshold}}$ is set to 0.005 in the algorithm. For the OFDM signal used in 5G systems, the

variance[1] of v_1^i can be calculated by the methods given in [21]–[23]

$$\sigma^2_{v_1^i} = \mathrm{var}(v_1^i) = \frac{c^2 T_s^2}{8\pi^2 \cdot \mathrm{SNR}_i \cdot \sum\limits_{n \in \mathcal{N}_{\mathrm{PRS}}} p_n^2 \cdot n^2}, \tag{19}$$

where c is the speed-of-light, T_s is the OFDM symbol duration equivalent to inverse to the subcarrier spacing F_{sc}(i.e., $T_s = \frac{1}{F_{sc}}$), $\mathcal{N}_{\mathrm{PRS}}$ is the subset of positioning reference signal (PRS) pilot subcarriers, and p_n^2 is the relative power weight of the nth subcarrier.

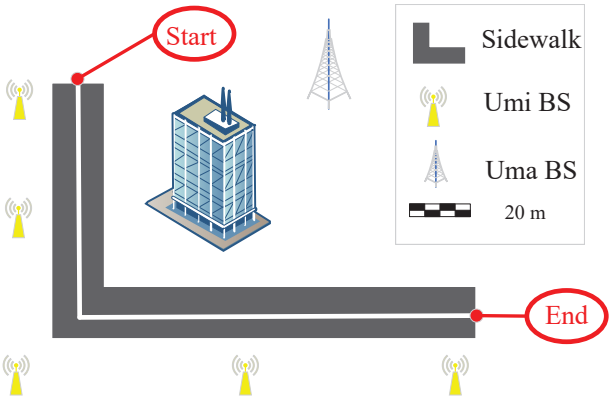

Fig. 2: UMi-street and UMa-street scenarios with the MT trajectory (solid white line) and BSs in 5G ultra-dense networks.

The error statistic is evaluated in the presence of NLOS. The channel impulse response (CIR) is simulated by ray-tracing [24]. A generic model for the simulated CIR is modeled as

$$h(\tau) = \sum_{L-1}^{l=0} \alpha_l \delta(\tau - \tau_l), \tag{20}$$

where L is the number of multipath components, α_l and τ_l are the relative attenuation and delay components, respectively, of the lth path with respect to the first path. Then the NLOS bias term v_2^i can be predicted based on the simulated CIR, and is expressed as [24]

$$v_2^i = \frac{c(\sin(\frac{\pi}{2N_a}))^3}{4\pi F_{sc} \cos(\frac{\pi}{2N_a})}(\chi_1 + \chi_2), \tag{21}$$

where N_a denotes the number of active subcarriers, χ_1 and χ_2 are the biases due to multipath as introduced in [24] depending on the geometric properties of the CIR.

A. Simulation in 5G Ultra-dense Network Scenario

Fig. 3 shows a plot of σ_{v_1} as a function of the carrier-to-noise ratio C/N_0 by using different 5G system bandwidths, and considering the possible range of C/N_0 in the 5G ultra-dense network scenario. Let us define the C/N_0 limits for two main network designs with high and low intersite distance (ISD), i.e., d_{MB} equal to 116 m and 5 m, respectively. The 5G ultra-dense network scenarios are defined using the predefined parameters in TABLE I. In the first case, the maximum path losses are assumed. As it is shown in Fig. 3, by utilizing the ultra-dense network scenario path loss model [25], a path loss is around 132.59 dB for $d_{\mathrm{MB}} = 120\,\mathrm{m}$ at $f = 30\,\mathrm{GHz}$. Using $P_{max} = 43\,\mathrm{dBm}$ and $\mathrm{SF} = 2\sigma_{\mathrm{SF}}$, the C/N_0 limit is at 72.91 dB-Hz, which only allows to achieve a target accuracy of 30 cm with a signal bandwidth higher than 50 MHz. In the second case, minimum path losses are considered. By utilizing the ultra-dense network scenario path loss model [25], a path loss is around 83.75 dB for $d_{\mathrm{MB}} = 5\,\mathrm{m}$ at $f = 30\,\mathrm{GHz}$. Thus, with maximum power $P_{max} = 43\,\mathrm{dBm}$ and $\mathrm{SF} = 2\sigma_{\mathrm{SF}}$, the C/N_0 limit is equal to 121.15 dB-Hz, i.e., the target accuracy can be achieved with any signal bandwidth. These two C/N_0 limits are shown in Fig. 3. It is observed that due to the large transmission bandwidth of higher N_{RB}, the standard deviation of code phase error is two orders of magnitude lower compared to lower N_{RB}.

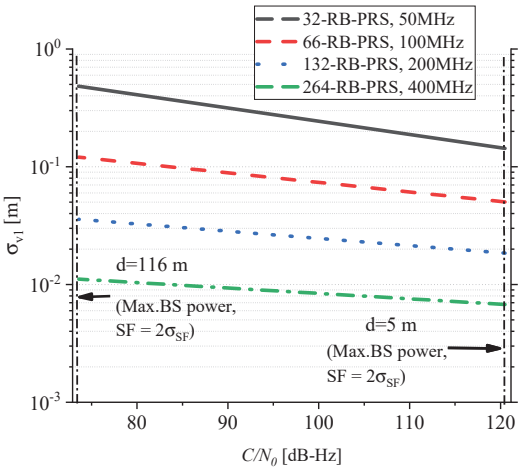

Fig. 3: Plot of σ_{v_1} as a function of the carrier-to-noise ratio C/N_0 by using different 5G system bandwidths, and considering the possible range of C/N_0 in the 5G ultra-dense network scenario.

Fig. 4 illustrates localization errors along the path. Fig. 5 illustrates the cumulative distribution function (CDF) of localization error. From Fig. 6 and Fig. 5, we see that the proposed RPF algorithm can achieve one-meter level positioning accuracy even under LOS/NLOS environment conditions in 5G ultra-dense network scenarios. This is because we have built an effective LOS/NLOS feasible region to filter unsuitable particles. It is observed that IMM-EKF has better positioning performance than PF. The significance of IMM theory is to combine the switching of the LOS and the

[1]According to [21], (19) is obtained from the Cramér-Rao lower bound (CRLB) of the time delay based on the time of arrival (TOA) estimation.

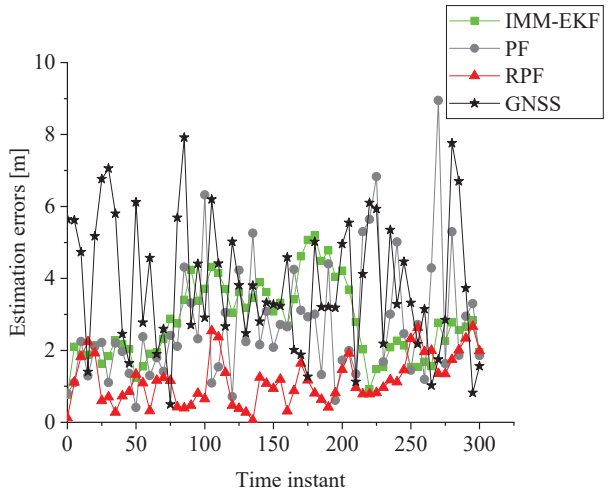

Fig. 4: Localization error along the path.

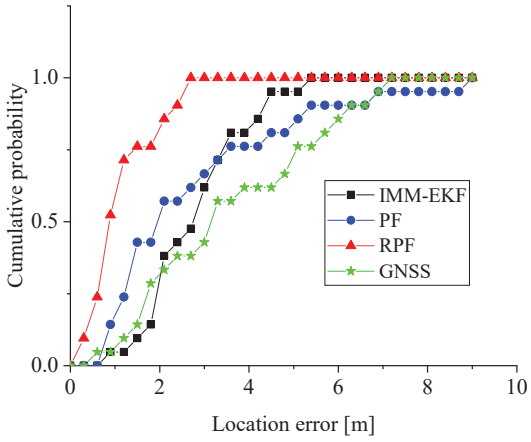

Fig. 5: The CDF of localization error.

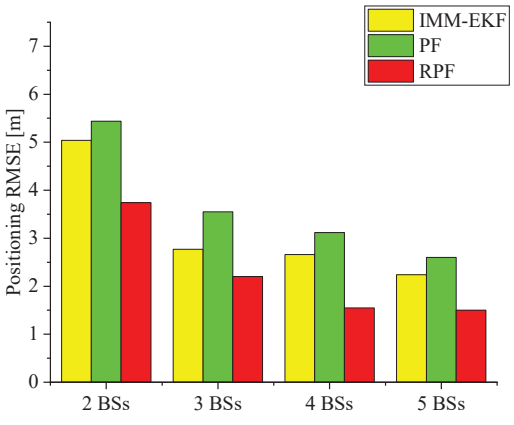

Fig. 6: RMSEs for all positioning methods with different number of BSs.

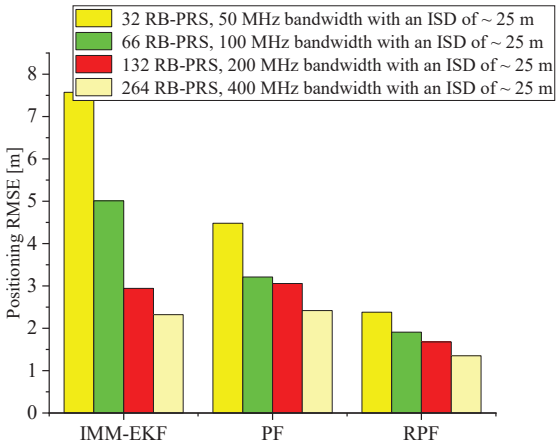

Fig. 7: RMSEs for all positioning methods under different simulation numerologies with an ISD of 25 m.

NLOS. Then the problem of positioning estimation is converted to a nonlinear filtering of jump Markov systems with two independent switching parameters. Hence, IMM-EKF is more robust than PF in mixed LOS/NLOS environments.

The results from the comprehensive numerical evaluations are illustrated in Fig. 6. Fig. 6 illustrates that positioning performance improves when ranging measurements are fused from more BSs compared to the scenario with fewer BSs. Although there exists interference between BSs, more effective observations are also helpful for the improvement of positioning accuracy. Fig. 7 shows RMSEs for all positioning methods under different simulation numerologies with an ISD of 25 m. It is shown that due to the large transmission bandwidth of higher N_{RB}, the standard deviation of the measurement noise error is two orders of magnitude lower compared to lower N_{RB}.

IV. Conclusion

In this paper, we proposed the key enabling technology for GNSS/5G collaborative navigation in urban environments. First, we derived the posterior belief over the state space conditioned on the given ranging measurements (LOS/NLOS) and GNSS velocity. Then, a RPF algorithm for urban environments was proposed to estimate the sight state and position of the MT. Next, 5G measurement error statistics in a LOS environment and in the presence of NLOS were presented. Finally, comprehensive performance evaluations were conducted in 5G ultra-dense networks. Simulation results demonstrated that meter-scale positioning could be achieved in LOS/NLOS using the proposed RPF technique.

Acknowledgment

This work was sponsored by the National Natural Science Foundation of China under Grant 62271352, the Shanghai Science and Technology Innovation Action Plan Project No.

TABLE I: The Environment Parameters of the 5G Ultra-dense Networks

Parameters [15]	Value		Parameters [15]	Value	
	UMi	UMa		UMi	UMa
Shadow fading standard deviation σ_{SF}	6.5 dB	6.5 dB	Bandwidth B	100 MHz	25 MHz
Frequency f	30 GHz	3 GHz	Number of resource blocks for subcarrier N_{RB}	66	65
Number of active subcarriers N_a	788	776	Subcarrier spacing F_{sc}	120 kHz	30 kHz

21220713100, the Natural Science Foundation of Shanghai under Grant 22ZR1465100, and the Shanghai Automobile Foundation under Grant 1905 (Corresponding author: Rui Wang).

REFERENCES

[1] B. Panchal, K. Subramanian, and S. E. Talole, "Robust missile autopilot design using two time-scale separation," *IEEE Trans. Aerosp. Electron. Syst.*, vol. 54, DOI 10.1109/TAES.2018.2796654, no. 3, pp. 1499–1510, 2018.

[2] B. Kürkçü and C. Kasnakoğlu, "Robust autopilot design based on a disturbance/uncertainty/coupling estimator," *IEEE Trans. Control Syst. Technol.*, vol. 27, no. 6, pp. 2622–2629, 2018.

[3] Z. Deng, P. Wang, T. Liu, Y. Cao, and B. Wang, "Foot-mounted pedestrian navigation algorithm based on BOR/MINS integrated framework," *IEEE Trans. Ind. Electron.*, vol. 67, no. 5, pp. 3980–3989, 2019.

[4] K. Wen, K. Yu, Y. Li, S. Zhang, and W. Zhang, "A new quaternion Kalman filter based foot-mounted IMU and UWB tightly-coupled method for indoor pedestrian navigation," *IEEE Trans. Veh. Technol.*, vol. 69, no. 4, pp. 4340–4352, 2020.

[5] N. Zhu, J. Marais, D. Bétaille, and M. Berbineau, "GNSS position integrity in urban environments: A review of literature," *IEEE Trans. Intell. Transp. Syst.*, vol. 19, no. 9, pp. 2762–2778, 2018.

[6] M. Witrisal, Klaus *et al.*, "High-accuracy localization for assisted living: 5G systems will turn multipath channels from foe to friend," *IEEE Signal Process. Mag.*, vol. 33, no. 2, pp. 59–70, 2016.

[7] C. Koivisto, Mike *et al.*, "Joint device positioning and clock synchronization in 5G ultra-dense networks," *IEEE Trans. Wirel. Commun.*, vol. 16, no. 5, pp. 2866–2881, 2017.

[8] F. Wen, J. Kulmer, K. Witrisal, and H. Wymeersch, "5G positioning and mapping with diffuse multipath," *IEEE Trans. Wirel. Commun.*, vol. 20, no. 2, pp. 1164–1174, 2021.

[9] H. Kim, K. Granstrom, L. Gao, G. Battistelli, S. Kim, and H. Wymeersch, "5G mmWave cooperative positioning and mapping using multi-model PHD filter and map fusion," *IEEE Trans. Wirel. Commun.*, vol. 19, no. 6, pp. 3782–3795, 2020.

[10] O. Kanhere and T. S. Rappaport, "Position location for futuristic cellular communications: 5G and beyond," *IEEE Commun. Mag.*, vol. 59, no. 1, pp. 70–75, 2021.

[11] L. Yin, Q. Ni, and Z. Deng, "A GNSS/5G integrated positioning methodology in D2D communication networks," *IEEE J. Sel. Areas Commun.*, vol. 36, no. 2, pp. 351–362, 2018.

[12] S.-C. Lin and I. F. Akyildiz, "Dynamic base station formation for solving NLOS problem in 5G millimeter-wave communication," in *Proc. IEEE INFOCOM*, pp. 1–9. IEEE, 2017.

[15] 3GPP, "Study on NR positioning support," 3rd Generation Partnership Project (3GPP), Technical report (TR), 03 2019.

[13] Y. Wang, K. Gu, Y. Wu, W. Dai, and Y. Shen, "NLOS effect mitigation via spatial geometry exploitation in cooperative localization," *IEEE Trans. Wirel. Commun.*, vol. 19, no. 9, pp. 6037–6049, 2020.

[14] W. Li and Y. Jia, "Location of mobile station with maneuvers using an imm-based cubature kalman filter," *IEEE Trans. Ind. Electron.*, vol. 59, DOI 10.1109/TIE.2011.2180270, no. 11, pp. 4338–4348, 2012.

[16] O. Kanhere and T. S. Rappaport, "Position location for futuristic cellular communications: 5G and beyond," *IEEE Commun. Mag.*, vol. 59, no. 1, pp. 70–75, 2021.

[17] S. He and S.-H. G. Chan, "Wi-fi fingerprint-based indoor positioning: Recent advances and comparisons," *IEEE Commun. Surv. Tutor.*, vol. 18, DOI 10.1109/COMST.2015.2464084, no. 1, pp. 466–490, 2016.

[18] J. Wang, Q. Gao, Y. Yu, H. Wang, and M. Jin, "Toward robust indoor localization based on Bayesian filter using chirp-spread-spectrum ranging," *IEEE Trans. Ind. Electron.*, vol. 59, no. 3, pp. 1622–1629, 2011.

[19] S. K. Rechkemmer, X. Zang, A. Boronka *et al.*, "Utilization of smartphone data for driving cycle synthesis based on electric two-wheelers in shanghai," *IEEE Trans. Intell. Transp. Syst.*, vol. 22, no. 2, pp. 876–886, 2021.

[20] J. M. Pak, C. K. Ahn, Y. S. Shmaliy, and M. T. Lim, "Improving reliability of particle filter-based localization in wireless sensor networks via hybrid particle/fir filtering," *IEEE Trans. Ind. Inform.*, vol. 11, no. 5, pp. 1089–1098, 2015.

[21] J. A. del Peral-Rosado *et al.*, "Feasibility study of 5G-based localization for assisted driving," in *2016 International conference on localization and GNSS (ICL-GNSS)*, pp. 1–6. IEEE, 2016.

[22] Q. Liu, R. Liu, Z. Wang, and Y. Zhang, "Simulation and analysis of device positioning in 5G ultra-dense network," in *in 2019 15th Int. Wirel. Commun. Mob. Comput. Conf.(IWCMC)*, pp. 1529–1533. IEEE, 2019.

[23] O. Renaudin, J. A. L. Salcedo, G. Seco-Granados, I. Lapin, F. Zanier, and L. Ries, "TOA Error Bounds for Positioning in 5G New Radio Networks," in *Proceedings of the 34th International Technical Meeting of the Satellite Division of The Institute of Navigation (ION GNSS+ 2021)*, pp. 2940–2956, 2021.

[24] K. Shamaei and Z. M. Kassas, "Receiver design and time of arrival estimation for opportunistic localization with 5G signals," *IEEE Trans. Wirel. Commun.*, vol. 20, no. 7, pp. 4716–4731, 2021.

[25] K. Haneda, J. Zhang *et al.*, "5G 3GPP-like channel models for outdoor urban microcellular and macrocellular environments," in *2016 IEEE 83rd vehicular technology conference (VTC spring)*, pp. 1–7. IEEE, 2016.